

- 16, 137.
3. (a) Di Salvo, F. J. *Surf. Sci.* **1976**, *58*, 297. (b) Monceau, P., Ed.; D. Reidel: Dordrecht, *Electronic Properties of Inorganic Quasi-One-Dimensional Compounds*; 1985; Parts 1, 2.
 4. Wells, A. F. *Structural Inorganic Chemistry*; 5th Ed.; Oxford University Press: New York, U.S.A., 1984; p 11 00.
 5. Rao, C. N. R.; Gopalakrishnan, Frsj. *New directions in solid state chemistry*; Cahn, R. W., Ed.; Cambridge University Press: Cambridge, 1986; Chap. 6.
 6. Keszler, D. A.; Ibers, J. A. *J. Solid State Chem.* **1984**, *52*, 73.
 7. Sunshine, S. A.; Keszler, D. A.; Ibers, J. A. *Acc. Chem. Res.* **1987**, *20*, 395.
 8. Keszler, D. A.; Ibers, J. A.; Shang, M.; Lu, J. *J. Solid State Chem.* **1985**, *57*, 68.
 9. Squattrito, P. J.; Sunshine, S. A.; Ibers, J. A. *J. Solid State Chem.* **1986**, *64*, 261.
 10. Sunshine, S. A.; Ibers, J. A. *Inorg. Chem.* **1985**, *25*, 43 55.
 11. The analytical method as employed in the Northwestern absorption program, AGNOST, was used for the absorption correction (de Meulenaer, J.; Tompa, H. *Acta Crystallogr.* **1965**, *19*, 1014.).
 12. Sheldrick, G. M. *Acta Cryst.* **1990**, *A46*, 467.
 13. Sheldrick, G. M. *SHELXL 93, Program for the Refinement of Crystal Structures*; University of Göttingen, 1993.
 14. Lee, Young-Ju; Jung, Chan-Sun; Sin, Hee-Kyoon. *J. Kor. Phys. Soc.* **1993**, *26*, 503.
 15. Rossi, A. R.; Hoffmann, R. *Inorg. Chem.* **1975**, *14*, 365.
 16. Epstein, A. J.; Conwell, E. M.; Sandman, D. J.; Miller, J. S. *Solid State Commun.* **1977**, *23*, 355.
 17. Epstein, A. J. *Molecular Metals*; Hatfield, W. E., Ed.; Plenum Press: New York, U.S.A., 1979; p 155.

A Theory on Phase Behaviors of Diblock Copolymer/Homopolymer Blends

Kyung-Sup Yoon and Hyungsuk Pak*

Department of Chemistry, Seoul National University, Seoul 151-742, Korea

Received July 6, 1995

The local structural and thermodynamical properties of blends A-B/H of a diblock copolymer A-B and a homopolymer H are studied using the polymer reference interaction site model (RISM) integral equation theory with the mean-spherical approximation closure. The random phase approximation (RPA)-like static scattering function is derived and the interaction parameter is obtained to investigate the phase transition behaviors in A-B/H blends effectively. The dependences of the microscopic interaction parameter and the macrophase-microphase separation on temperature, molecular weight, block composition and segment size ratio of the diblock copolymer, density, and concentration of the added homopolymer, are investigated numerically within the framework of Gaussian chain statistics. The numerical calculations of site-site interchain pair correlation functions are performed to see the local structures for the model blends. The calculated phase diagrams for A-B/H blends from the polymer RISM theory are compared with results by the RPA model and transmission electron microscopy (TEM). Our extended formal version shows the different feature from RPA in the microscopic phase separation behavior, but shows the consistency with TEM qualitatively. Scaling relationships of scattering peak, interaction parameter, and temperature at the microphase separation are obtained for the molecular weight of diblock copolymer. They are compared with the recent data by small-angle neutron scattering measurements.

Introduction

The interaction parameter (χ parameter or interaction energy)¹⁻⁶ is considered as a gauge of interaction between the polymer chains and as a *black box* in the field of polymer science. χ parameter associated with the enthalpy of mixing is an important characteristic one in high molecular weight polymer systems. A great flux of activities thus has been pursued to understand the fundamental concept of χ parameter. Such χ parameter also can be used to predict phase separations because it governs phase behaviors of polymer blends. The phase separation behaviors are common in polymeric

materials, particularly when two different polymers are present as the form of blends and/or block copolymers.

Many theoretical and experimental studies have been used in conjunction with scattering data⁷⁻¹⁹ and Monte Carlo (MC) simulations^{20,21} to provide important tools in studies of thermodynamic interactions in polymer mixtures. Among these theoretical studies the most typical two models are the well known Flory-Huggins lattice model (FHLM)¹ and the random phase approximation (RPA) model² developed initially by de Gennes. Flory-Huggins χ parameter is only treated as a function of temperature, $\chi \propto 1/T$. Many experimental results show that χ parameter is affected by molecular weight and

composition as well as temperature. Thus χ parameter from FHLM does not give the desired polymer blend information. In particular, polymer blends with the diblock copolymer can exhibit a variety of phase separation behavior, that is, microphase separation, where domains of two blocks are subdivided into the microdomains, and macrophase one. In these cases χ parameter depends on temperature, composition and segment size ratio of blocks in the diblock copolymer, compressibility, molecular weight, and concentration of the added homopolymer, etc. The RPA model used to interpret the scattering data has been applied to investigate the phase behaviors of polymer blends. This is derived by utilizing the linear response theory in conjunction with the mean-field treatment of interchain interactions and the intrinsic assumption of incompressibility. As the result of inadequacy of such an incompressible model used to extract χ parameter, the RPA model also does not give the proper prediction of essential informations of blends.¹⁷

Recently the off-lattice integral equation theory (IET) by Curro and Schweizer²² is developed to understand the structure and thermodynamics of binary polymer blends. In particular, this theory shows the dependence of χ parameter on the structure at the monomer level and even the wave vector in connection with scattering experiments. This approach, the so-called polymer *reference interaction site model* (RISM) theory, to describe binary homopolymer blends is based on the RISM IET originally proposed by Chandler and co-workers.²³⁻²⁵ Here the RISM theory has been very successful for describing small molecular liquids and has been successfully applied to interpret the molecular structure factors measured by scattering techniques,²⁶ the structure of a polyatomic fluid sorbed by a quenched amorphous material,²⁷ and later the behavior of molecular and polymeric fluids adsorbed within microporous solids.²⁸ The RISM theory is first formulated in a fashion which renders the high polymer melt problem tractable by Curro and co-workers.²⁹⁻³¹

As already stressed, polymer blends of diblock copolymer A-B and homopolymer H exhibit unique phase behaviors. Within frames of the Edwards Hamiltonian method (EHM)¹⁰ and the RPA,¹¹ the A-B/H blend systems have been studied for investigating phase transition and separation behaviors. In recent years Benoit and co-workers³² formulated the static scattering theory for multicomponent polymers and/or copolymer systems by applying the RPA and the Ornstein-Zernike (OZ) equation.^{24,25}

While on the other hand, in the framework of the polymer RISM theory, relatively little work has been done to describe the multicomponent polymer blend systems containing the block copolymer as an important component. In this paper the local structure and thermodynamics of blends A-B/H of a diblock copolymer A-B and a homopolymer H are studied to understand the phase separation behaviors by using χ parameter derived at the microscopic level from the polymer RISM theory. Therefore, to extract the proper χ parameter (or χ function), the extended formal version of the polymer RISM IET is presented with the mean-spherical approximation (MSA)^{22,24,25} closure. The dependences of the effective microscopic χ parameter, the macro- and microphase separation, and the static structure factor on temperature, composition and segment size ratio of the diblock copolymer, mole-

cular weight, packing fraction, and concentration of the homopolymer particularly, are investigated numerically within the Gaussian chain statistics. Then our calculated results are compared with small-angle X-ray scattering (SAXS)¹³ and small-angle neutron scattering (SANS)^{15,16} data, phase diagrams by conventional RPA calculations,¹¹ and also transmission electron microscopy (TEM) studies.³³ Finally, the site-site interchain pair correlation functions (PCFs), $g_{MM}(r)$, are calculated to see the local structure for the model blend.

Polymer RISM Theory for A-B/H Blend System

In all works described below, it is assumed that polymer chains and blocks of segment number density ρ_M , each composed of N_M segments, follow the Gaussian chain statistics. Each interaction site is characterized by a hard core diameter, d_M ($=d_{MM}$), and a statistical segment length, σ_M , of species M.

The system under consideration consists of a mixture of homopolymer H having the volume fraction ϕ_H , and diblock copolymer A-B having the volume fraction ϕ_V for the block A. The volume fractions of diblock copolymer and block A in the mixture equal to $(1-\phi_H)$ and $\phi_V(1-\phi_H)$, respectively. The homopolymer consists of the same segments as that of block A in the diblock copolymer, i.e., $\sigma_H = \sigma_A$, and $d_H = d_A$, the so-called *pseudo-two-components* blend system.

We consider the simple *tangent hard-sphere model* ($\sigma_M/d_M \rightarrow 1$), and thus the local structural parameter is characterized by the stiffness ratio as follows:

$$\gamma = \frac{\sigma_B}{\sigma_A} = \frac{d_B}{d_A} \quad (1)$$

The total segment volume or packing fraction that is the ratio with respect to the close-packed volume, is defined by

$$\eta = \rho_A \bar{v}_A + \rho_B \bar{v}_B + \rho_H \bar{v}_H \quad (2)$$

where \bar{v}_M is the average segment volume of species M. In the incompressible close-packed system, η is equal to unity, but is not equal to unity in the off-lattice case such as this model. The segment volume is defined by

$$\bar{v}_M = \frac{1}{6} \pi d_M^3 (1 - \Delta_M) \quad (3)$$

where Δ_M represents the overlap volume fraction suggested by Schweizer and Curro³⁰ which can be caused by the unphysical overlaps between the non-bonded sites for considering the single chain interaction. No consideration for the self-avoiding walks between hard spheres in the calculation of the intramolecular distribution function leads to the increasing of η .

Two segment volume ratios are defined by

$$R_{AB} = \frac{\bar{v}_A}{\bar{v}_B} = \frac{d_A^3(1-\Delta_A)}{d_B^3(1-\Delta_B)} = \frac{(1-\Delta_A)}{\gamma^3(1-\Delta_B)} \quad (4a)$$

$$R_{AH} = \frac{\bar{v}_A}{\bar{v}_H} = \frac{(1-\Delta_A)}{(1-\Delta_H)} \quad (4b)$$

The homopolymer is considered as the same segment as that of the block A in the diblock copolymer, but R_{AH} is not unity because of the different number of segments, and

consequently the different Δ_M .

The relative segment volume fraction of species of M is defined by

$$\phi_M = \rho_M \bar{v}_M / \eta \quad (5)$$

From Eqs. (1)-(5) the interaction segment number density, $\rho_M d_M^3$, is given by

$$\rho_{AH} d_A^3 = \frac{\delta \eta \phi_{AH}}{\pi(1 - \Delta_{AH})} \quad (6a)$$

$$\rho_B d_B^3 = \frac{\delta \eta \phi_B}{\gamma^2 \pi(1 - \Delta_B)} \quad (6b)$$

and thus the site number density ratio is simply expressed as

$$\frac{\rho_M}{\rho_A} = \frac{\phi_M}{\phi_A} R_{AM} \quad (M=H, B) \quad (7)$$

Polymer RISM Equations with MSA Closure. The polymer RISM theory is designed to calculate the intermolecular PCF, $g_{\alpha\beta MM'}(r)$, between sites α and β on each chain of two species M and M' interacting through the intermolecular site-site pair potential, $u_{\alpha\beta MM'}(r)$, the intermolecular site-site total correlation function, $h_{\alpha\beta MM'}(r) \equiv g_{\alpha\beta MM'}(r) - 1$, and the corresponding intermolecular direct correlation function (DCF), $C_{\alpha\beta MM'}(r)$, defined by the generalized OZ non-linear integral equations (NIEs).

For a polymer chain composed of identical sites in homopolymer melts²⁹⁻³¹ and a binary homopolymer blend,²² OZ-equations reduce to a single NIE and a set of three-coupled NIEs, respectively by neglecting the chain end effects and considering the chain-averaged approximation over all site pairs. The diblock copolymer A-B and the homopolymer H blend with H containing the same segment as that of block A can be considered as A/B type blend system. The same conceptual approximation as that of a binary homopolymer blend is used by neglecting chain end effects, and additionally block-joint effects of diblock copolymer chains on DCFs. Moreover, by considering the block-average approximation, the polymer RISM equations are expressed by a set of three-coupled NIEs.

The total correlation between two sites α on a polymer of species M and β of species M' is described by two types of correlation functions. One is the direct correlation part, and the other is indirect correlation part which is additionally propagated *via* increasing large number of polymer molecules and/or blocks in the diblock copolymers and many other routes. By summing over all $\{\alpha, \beta\}$ pairs, the total correlation function between polymer chains is given compactly in Fourier transform space in terms of a non-linear matrix equation as

$$\begin{aligned} \hat{\mathbf{H}}(k) &= \hat{\Omega}(k) \cdot \hat{\mathbf{C}}(k) \cdot [\hat{\Omega}(k) + \hat{\mathbf{H}}(k)] \\ &= [\hat{\mathbf{1}} - \hat{\Omega}(k) \cdot \hat{\mathbf{C}}(k)]^{-1} \cdot \hat{\Omega}(k) \cdot \hat{\mathbf{C}}(k) \cdot \hat{\Omega}(k) \end{aligned} \quad (8)$$

where the elements of 2×2 matrices are defined by

$$\hat{H}_{MM'}(k) = \rho_M \rho_{M'} \hat{h}_{MM'}(k) \quad (9a)$$

$$\hat{\Omega}_{MM'}(k) = \frac{\rho}{N} \sum_{\alpha=1}^{NM} \sum_{\beta=1}^{NM'} \hat{\omega}_{\alpha\beta MM'}(k) \quad (9b)$$

and $\rho = \rho_M + \rho_{M'}$ and $N = N_M + N_{M'}$.

The polymer RISM theory needs the closure condition to determine the PCF from the relation between unknown DCF and total correlation function. Many applications have been usually focused on the MSA closure which the pair potential consists of a hard sphere interaction plus an attractive tail, $u_{MM'}(r) = u_{MM'}^0(r) + V_{MM'}(r)$. For the hard sphere chain model, the exact hard core condition gives

$$H_{MM'}(r) = -\rho_M \rho_{M'} \quad r < d_{MM'} \quad (10a)$$

$$d_{MM'} = \frac{1}{2}(d_M + d_{M'}) \quad (10b)$$

where $d_{MM'}$ is the closest distance of the possible approach between two sites of polymer types M and M'. The DCF is given asymptotically by

$$C_{MM'}(r) \equiv -\beta V_{MM'}(r) \quad r > d_{MM'} \quad (10c)$$

A modified Lennard-Jones 6-12 attractive potential in Eq. (10c) was used to model the interaction between two sites on different chains and/or blocks:

$$V_{MM'}(r) = \epsilon_{MM'} [(r/d_{MM'})^{-12} - 2(r/d_{MM'})^{-6}] \quad r \geq d_{MM'} \quad (11)$$

where $\epsilon_{MM'}$ is the interaction energy parameter.

The three-coupled OZ-NIEs of Eq. (8) and the MSA closure of Eq. (10) make up the polymer RISM equations for the polymer blend systems.

Intramolecular Structure Factor. The structural informations of polymers enter the polymer RISM equations solely through the single chain distribution functions.²² For a homopolymer or a block chain, $\omega_{MM}(r) \equiv \omega_M(r)$ is defined by

$$\omega_M(r) = \frac{1}{N_M} \sum_{ij}^{NM} \omega_{ij}(r; M) \quad (12)$$

where $\omega_{ij}(r; M)$ is the probability that a pair of sites i and j on the same chain or block are separated by a distance r . For a fully flexible linear Gaussian chain, the single chain structure factor, which is given by Fourier transformation of Eq. (12), reduces to

$$\begin{aligned} \hat{\omega}_M(k) &= \frac{1}{N_M} \sum_{ij}^{NM} \exp(-k^2 \sigma_M^2 |i-j|/6) \\ &= (1-f_M)^{-2} \left[1 - f_M^2 - \frac{2f_M}{N_M} + \frac{2f_M^{NM+1}}{N_M} \right] \end{aligned} \quad (13)$$

where

$$f_M = \exp(-k^2 \sigma_M^2/6) \quad (14)$$

While for a diblock copolymer the single chain distribution function, $\omega_{AB}(r)$, is given by

$$\omega_{AB}(r) = \frac{1}{N_C/2} \sum_{i \in A} \sum_{j \in B} \omega_{ij}(r; A, B) \quad (15)$$

where $\omega_{ij}(r; A, B)$ is the bond probability that a site i of block type A and a site j of B are separated by a distance r . The intramolecular structure for a diblock copolymer is thus derived as

$$\hat{\omega}_{AB}(k) = \frac{2}{N_C} \sum_{i=1}^{N_A} \sum_{j=1}^{N_B} \exp(-k^2 \sigma_A^2 i/6) \exp(-k^2 \sigma_B^2 j/6)$$

$$= \frac{2}{N_C} \frac{1-f_A^{NA}}{1-f_A} f_{NB} \frac{1-f_B^{NB}}{1-f_B} \quad (16)$$

where f_A and f_B have the same form as Eq. (14).

The total intramolecular structure factors, $\hat{\Omega}_{MM}(k)$ in Eq. (8), for A-B/H blend system are given more distinctly by

$$\hat{\Omega}_{AA}(k) = \rho_A \hat{\omega}_A(k) + \rho_H \hat{\omega}_H(k) \quad (17a)$$

$$\hat{\Omega}_{BB}(k) = \rho_B \hat{\omega}_B(k) \quad (17b)$$

$$\hat{\Omega}_{AB}(k) = \frac{1}{2} \rho_C \hat{\omega}_{AB}(k) \quad (17c)$$

where ρ_C is the total segment number density of the A-B diblock copolymer, i.e., $\rho_C = \rho_A + \rho_B$.

Solution of Polymer RISM Equations. The numerical calculations of the polymer RISM equations, Eqs. (8) and (10) can be performed with a variational principle of the scheme originally proposed by Lowden and Chandler.²³ In order to proceed this method, the DCFs inside the hard core are approximated by a third degree of polynomial in r , a linear combination of suitable basis functions:^{23,34}

$$C_{MM}(r) = H(r - d_{MM}) \sum_{i=1}^4 a_i^{MM} \left(\frac{r}{d_{MM}} - 1 \right)^{i-1} \quad r < d_{MM} \quad (18)$$

where a_i^{MM} are three sets of expansion coefficients that must be determined self-consistently by solving a set of 12-coupled non-linear equations.

The basis functions are independent of each other, thus the corresponding hard core condition closure equation, Eq. (10a), is rewritten as

$$\rho_M \rho_M \int dr [1 + h_{MM}(r)] \left(\frac{r}{d_{MM}} - 1 \right)^{i-1} = 0 \quad (19)$$

This solution equation can be transformed into k -space using the Parseval's relation.²⁶ The resulting equation is derived by using the dimensionless variable as convenient forms for the calculation of 12-expansion coefficients, a_i^{MM} .

$$2\pi^2 [(\rho_M \rho_M)^{1/2} d_A^3] \frac{\partial [(\rho_M \rho_M)^{1/2} \hat{C}_{MM}(0)]}{\partial a_i^{MM}} + \int dx x^2 \frac{\partial [(\rho_M \rho_M)^{1/2} \hat{C}_{MM}(x)]}{\partial a_i^{MM}} \frac{\hat{H}_{MM}(x)}{(\rho_M \rho_M)^{1/2}} = 0 \quad (20)$$

where the reduced variable $x = kd_A$.

From the three-coupled OZ-NIEs in terms of 2×2 matrices, Eq. (8), the partial structures of total intermolecular correlation functions are obtained in terms of the intramolecular, Eq. (17), and the direct intermolecular structure factors with notations without the variable as

$$\frac{\hat{H}_{AA}(x)}{\rho_A} = \frac{1}{\Lambda} \left[\Phi_{AH}(1 - \hat{\Lambda} - \hat{\omega}_B \rho_B \hat{C}_{BB}) + \frac{1}{4} \Phi_{AB}^2 \hat{\omega}_{AB}^2 \rho_B \hat{C}_{BB} \right] \quad (21a)$$

$$\frac{\hat{H}_{BB}(x)}{\rho_B} = \frac{1}{\Lambda} \left[\hat{\omega}_B(1 - \hat{\Lambda}) - \Phi_{AH} \hat{\omega}_B \rho_A \hat{C}_{AA} + \frac{1}{4} \Phi_{AB}^2 \hat{\omega}_{AB}^2 \rho_B \hat{C}_{AA} \right] \quad (21b)$$

$$\frac{\hat{H}_{AB}(x)}{(\rho_A \rho_B)^{1/2}} = \frac{1}{\Lambda} \left[\frac{1}{2} \Phi_{AB} \hat{\omega}_{AB}(1 - \hat{\Lambda}) + \Phi_{AH} \hat{\omega}_B (\rho_A \rho_B)^{1/2} \hat{C}_{AB} - \frac{1}{4} \Phi_{AB}^2 \hat{\omega}_{AB}^2 (\rho_A \rho_B)^{1/2} \hat{C}_{AB} \right] \quad (21c)$$

where

$$\begin{aligned} \hat{\Lambda}(x) &= \det[\hat{1} - \hat{\Omega}(x) \cdot \hat{C}(x)] \\ &= 1 - \hat{\Omega}_{AA}(x) \hat{C}_{AA}(x) - \hat{\Omega}_{BB}(x) \hat{C}_{BB}(x) - 2 \hat{\Omega}_{AB}(x) \hat{C}_{AB}(x) \\ &\quad + \delta \hat{\Omega}(x) \delta \hat{C}(x) \end{aligned} \quad (22)$$

$$\delta \hat{\Omega}(x) = \hat{\Omega}_{AA}(x) \hat{\Omega}_{BB}(x) - \hat{\Omega}_{AB}^2(x) \quad (23)$$

$$\delta \hat{C}(x) = \hat{C}_{AA}(x) \hat{C}_{BB}(x) - \hat{C}_{AB}^2(x) \quad (24)$$

Three direct intermolecular structure factors, $\hat{C}_{MM}(x)$, which will be incorporated into Eq. (21), have the following form:

$$\begin{aligned} \hat{C}_{MM}(x)/4\pi d_{MM}^3 &= a_1^{MM} (-\cos \xi/\xi^2 + \sin \xi/\xi^3) \\ &= a_2^{MM} (-2/\xi^4 - 2\cos \xi/\xi^4 + \sin \xi/\xi^5) \\ &= a_3^{MM} (4/\xi^4 + 2\cos \xi/\xi^4 - 6\sin \xi/\xi^5) \\ &= a_4^{MM} (24/\xi^6 - 6/\xi^4 - 24\cos \xi/\xi^5 - \sin \xi/\xi^5) \end{aligned} \quad (25)$$

where the variable $\xi = kd_{MM}$ and in $\xi \rightarrow 0$ limit,

$$\hat{C}_{MM}(0) = \frac{\pi}{15} d_{MM}^3 (20a_1^{MM} - 5a_2^{MM} + 2a_3^{MM} - a_4^{MM}) \quad (26)$$

To obtain the solution of the polymer RISM equations, we first guess an initial set of 12-expansion coefficients in the DCFs of Eqs. (25) and (26), and independently calculate the intramolecular structures, Eq. (17). The total intermolecular structure factors, Eq. (21), are then calculated. These structure factors are incorporated into the non-linear coupled polymer RISM solution equation, Eq. (20). Thus new guesses for a_i^{MM} are determined by calculating Eq. (20) with the closure relations, Eq. (10). For obtaining new guesses for a_i^{MM} we make use of the iteration method based on the *MinPack-1* algorithm²⁵ which is very efficient in the non-linear equations. a_i^{MM} have orders of range from -10^{-6} to -10^{-1} in our full systems.³⁸

Intermolecular Pair Correlation Function. The site-site intermolecular PCFs give the indirect informations about the local structures of the polymer blend system. These PCFs can be obtained by the Fourier inversion of $\hat{H}_{MM}(k)$ calculated numerically through the 12-coupled NIEs, Eq. (20). Such a relation is defined by

$$\begin{aligned} \rho_M \rho_M [g_{MM}(r) - 1] &= H_{MM}(r) = \frac{1}{(2\pi)^3} \int d\mathbf{k} e^{-i\mathbf{k} \cdot \mathbf{r}} \hat{H}_{MM}(k) \\ &= \frac{1}{2\pi^2 r} \int dk k \sin(rk) \hat{H}_{MM}(k) \end{aligned} \quad (27)$$

Three independent PCFs for A-B/H blend system are then described by

$$g_{MM}(r_A) = 1 + \frac{1}{2\pi^2 [(\rho_M \rho_M)^{1/2} d_A^3] r_A} \int dx x \sin(r_A x) \frac{\hat{H}_{MM}(x)}{(\rho_M \rho_M)^{1/2}} \quad (28)$$

where the reduced separation is $r_A = r/d_A$ and \hat{H}_{MM} is defined by Eq. (21).

Within the Gaussian chain statistics, the PCFs of the disordered polymer blends at high temperature does not show any characteristic structure. Usually the PCFs rapidly increase at first with increasing of the segmental separation and followed by a slow convergence to the uncorrelated value. Such a correlation hole effect for the polymer system is due to the intramolecular constraints and intermolecular excluded volume interactions, which are related with the

number of segments and the packing fraction, respectively.

Really the intrachain correlation functions must be determined self-consistently along with the DCFs and the total correlation functions through the OZ-NIEs, Eq. (8). But for simplicity, as described in Sec. 2.2, the single chain distribution functions are determined independently with the DCFs. Such an approximate method is not a good approach to the study of phase behaviors. As temperature decreases the inaccuracy is expected in the vicinity of the phase transition from the disordered phase to the ordered mesophase where non-Gaussian chain conformations have been observed. Thus non-Gaussian chain statistics³⁶ and self-consistent calculations³¹ of the single chain correlation functions and the DCFs also must be considered for obtaining the informations of local structures and phase behaviors in A-B/H blend systems.

Static Structure Factor and Interaction Parameter

Scattering theories and experiments have been applied to investigate a number of polymer fluids and blends over the past few years.^{7,19,32} The scattering function is related with the compressibility of the system and can be obtained experimentally from measurements of the cross-section as a function of the scattering angle.²⁴ By fitting the experimental data to the theoretical static structure functions, χ parameter can be extracted and used to study the phase separation and transition behaviors. In this section we derive the RPA-like static scattering function and χ function within the framework of the polymer RISM theory to study the phase separation behaviors, that is, macrophase separation and microphase separation due to the presence of the diblock copolymer in polymer blends.

The partial static structure factors relevant to scattering experiments, which are Fourier transforms of the density-density fluctuation correlation functions, are given in terms of the 2×2 matrices by

$$\hat{S}(k) = \hat{\Omega}(k) + \hat{H}(k) = [\hat{I} - \hat{\Omega}(k) \cdot \hat{C}(k)]^{-1} \cdot \hat{\Omega}(k) \quad (29)$$

Thus the inverse partial structure factors for the *pseudo*-two-components A-B/H blend system are given by

$$\hat{S}_{AA}^{-1}(k) = \frac{1}{\delta\hat{\Omega}(k)} [\hat{\Omega}_{BB}(k) - \delta\hat{\Omega}(k)\hat{C}_{AA}(k)] \quad (30a)$$

$$\hat{S}_{BB}^{-1}(k) = \frac{1}{\delta\hat{\Omega}(k)} [\hat{\Omega}_{AA}(k) - \delta\hat{\Omega}(k)\hat{C}_{BB}(k)] \quad (30b)$$

$$\hat{S}_{AB}^{-1}(k) = \frac{1}{\delta\hat{\Omega}(k)} [-\hat{\Omega}_{AB}(k) - \delta\hat{\Omega}(k)\hat{C}_{AB}(k)] \quad (30c)$$

where $\delta\hat{\Omega}(k)$ is defined by Eq. (23).

To extract χ parameter and compare it with the RPA, we employ the free energy functional integral method which was used by Leibler,⁷ Cruz and Sanchez,¹⁰ and Schweizer and Curro²² previously. The RPA is chiefly used by many experimentalists to obtain the scattering determined χ parameter, as above-mentioned, by fitting the scattering data.

The free energy functional of an inhomogeneous blend system with 2nd-order contribution in the presence of external field is given in terms of the partial density-density fluctuation

correlation function in the uniform and equilibrium mixture as

$$\beta\Delta F \cong \frac{1}{2} \sum_{MM'} \int dk \hat{S}_{MM'}^{-1}(k) \langle \delta\hat{\rho}_M(k) \rangle \langle \delta\hat{\rho}_{M'}(k) \rangle \quad (31)$$

where the segment density fluctuation of species M at a point r is

$$\delta\rho_M(r) \equiv \rho_M(r) - \rho_M \quad (32)$$

To obtain the concentration fluctuation part used to interpret the scattering data from the density fluctuation correlations, the segment density fluctuations are substituted with the volume fluctuation terms through the following relation:

$$\delta\phi_M(r) \propto \bar{v}_M \delta\rho_M(r) \quad (33)$$

and the incompressibility condition for total volume fraction of the polymers is used as

$$\sum_M \delta\phi_M(r) = 0 \quad (33b)$$

The resulting free energy functional with respect to the functional in the absence of the external potential yields

$$\beta\Delta F \cong \frac{1}{2} \sum_{MM'} \int dk \hat{S}_C^{-1}(k) |\delta\hat{\phi}_A(k)|^2 \quad (34)$$

where the concentration fluctuation part of the structure factor is finally defined in terms of the partial structure factors by

$$\hat{S}_C^{-1}(k) = \frac{\hat{S}_{AA}^{-1}(k)}{\bar{v}_A^2} + \frac{\hat{S}_{BB}^{-1}(k)}{\bar{v}_B^2} - 2 \frac{\hat{S}_{AB}^{-1}(k)}{\bar{v}_A \bar{v}_B} \quad (35)$$

Using the segment volume ratio, Eq. (4a), and the inverse partial static structure factors, Eq. (30), Eq. (35) is rewritten as the following form split into the single chain and the direct intermolecular structure factors:

$$\hat{S}_C^{-1}(k) = \frac{1}{\delta\hat{\Omega}} [\hat{\Omega}_{AA}(k) + R_{AB}^2 \hat{\Omega}_{BB}(k) + 2R_{AB} \hat{\Omega}_{AB}(k)] - [\hat{C}_{AA}(k) + R_{AB}^2 \hat{C}_{BB}(k) - 2R_{AB} \hat{C}_{AB}(k)] \quad (36)$$

By suitable procedures, the resulting *renormalized* RPA-like structure factor is given with the wave vector-dependent χ parameter by

$$\hat{S}_R^{-1}(k) = \eta(\bar{v}_A \bar{v}_B)^{1/2} \hat{S}_C^{-1}(k) = \hat{Q}(k) - 2\hat{\chi}(k) \quad (37)$$

where the function is given by

$$\hat{Q}(k) = \frac{R_{AB}^{1/2}(\Phi_A \hat{\omega}_A + R_{AH} \Phi_H \hat{\omega}_H) + R_{AB}^{-1/2} \Phi_B \hat{\omega}_B + (R_{AB}^{-1/2} \Phi_A + R_{AB}^{1/2} \Phi_B) \hat{\omega}_{AB}}{(\Phi_A \hat{\omega}_A + R_{AH} \Phi_H \hat{\omega}_H) \Phi_B \hat{\omega}_B - \frac{1}{4} (R_{AB}^{-1/2} \Phi_A + R_{AB}^{1/2} \Phi_B)^2 \hat{\omega}_{AR}^2} \quad (38)$$

and χ parameter in terms of the direct intermolecular structures has the same form for a binary polymer blend without a diblock copolymer

$$\hat{\chi}(k) = \frac{\rho/2}{R_{AB}^{-1/2}(\Phi_A + R_{AH} \Phi_H) + R_{AB}^{1/2} \Phi_B} [R_{AB}^{-1} \hat{C}_{AA}(k) + R_{AB} \hat{C}_{BB}(k) - 2\hat{C}_{AB}(k)] \quad (39)$$

In many other theoretical models, χ parameter is only a function of temperature or is treated with the constant value, while this χ parameter shows the dependence of the wave vector as well. The RPA form-like structure factor, Eq. (37), is renormalized with respect to the packing fraction. However χ function, Eq. (39), is still dependent on the compressibility of the system because of the dependence of expansion coefficients on the packing fraction in the direct intermolecular structures, Eq. (25).

In the absence of homopolymer, $\phi_H \rightarrow 0$, and the symmetric segmental volume $R_{AB} \rightarrow 1$ limit, that is, the diblock copolymer melt system, Eq. (37) reduces to

$$\hat{S}_R^{-1}(k) = \frac{\phi_A \hat{\omega}_A + \phi_B \hat{\omega}_B + \hat{\omega}_{AB}}{\phi_A \hat{\omega}_A \cdot \phi_B \hat{\omega}_B - \frac{1}{4} \hat{\omega}_{AB}^2} - 2\hat{\chi}(k) \quad (40)$$

and especially for the symmetric diblock copolymer melt system, $\phi_A = \phi_B$, one has the following simple form:

$$\hat{S}_R^{-1}(k) = \frac{2(\hat{\omega}_A + \hat{\omega}_B + 2\hat{\omega}_{AB})}{\hat{\omega}_A \hat{\omega}_B - \hat{\omega}_{AB}^2} - 2\hat{\chi}(k) \quad (41)$$

The A/B (or A/H) binary blend system which has been studied before by many polymer researchers is readily obtained from the usual system, ϕ_H (or ϕ_A) $\rightarrow 0$ and no intramolecular structure cross term, $\hat{\omega}_{AB} \rightarrow 0$, as follows:

$$\hat{S}_R^{-1}(k) = \frac{1}{R_{AB}^{1/2} \phi_A \hat{\omega}_A} + \frac{1}{R_{AB}^{-1/2} \phi_B \hat{\omega}_B} - 2\hat{\chi}(k) \quad (42)$$

Within the above-described polymer RISM theory with MSA closure, the DCFs consist of two terms. One is determined numerically by calculating the polymer RISM solution equations for $r < d_{MM}$, and the other comes from the closure, Eq. (10c), for $r > d_{MM}$. In the conventional FHLM χ parameter at high temperature ($T \rightarrow \infty$) limit does not have any meaning, but in this study it does not vanish and gives the significance as the purely entropy-driven quantity. Non-vanishment of χ parameter is due to the DCFs for $r < d_{MM}$, this may make a contribution to the phase separation behaviors of the multicomponent polymer blends. Thus χ parameter of the system, Eq. (39), is represented as the sum of two functions:

$$\hat{\chi}(x, T) = \hat{\chi}_{HT}(x) + \hat{\chi}_D(x, T) \quad (43)$$

where $x = kd_A$ as used in Eq. (20), the first term in the right-hand side is χ parameter at high temperature, and the second is the temperature and wave-vector dependent function. The two terms in Eq. (43) are represented by

$$\hat{\chi}_{HT}(x) = \rho C_x [R_{AB}^{-1} \hat{C}_{AA}(x) + R_{AB} \hat{C}_{BB}(x) - 2\hat{C}_{AB}(x)] \quad (44a)$$

$$\hat{\chi}_D(x, T) = \beta \rho C_x [2\hat{V}_{AB}(x, T) - R_{AB}^{-1} \hat{V}_{AA}(x, T) - R_{AB} \hat{V}_{BB}(x, T)] \quad (44b)$$

where $\hat{C}_{MM}(x)$ are the set of direct intermolecular structure factors inside the hard core diameter that can be obtained through the polymer RISM solution and the leading interaction constant is

$$C_x = \frac{1}{2} \frac{1}{R_{AB}^{-1/2}(\phi_A + R_{AH}\phi_H) + R_{AB}^{1/2}\phi_B} \quad (45)$$

In the range of $r > d_{MM}$, the interaction energy parameters

in a modified Lennard-Jones 6-12 potentials, Eq. (11), used to the DCFs are related with the temperature-dependence of χ parameter through the relation of $\epsilon_{MM} \propto 1/T$. For a usual specific symmetric interaction choice,^{22,37,39} which is reasonable at high density of polymer blends, the interaction energy parameters are treated as $\epsilon_{AA} = \epsilon_{BB} = 0$ and $\epsilon_{AB} < 0$. From the simplified condition, the interaction between unlike segments is given by

$$\beta \rho \hat{V}_{AB}(x, T) = -\frac{4\pi}{x} (\rho d_A^3) \left[\frac{1}{2}(1+\gamma) \right]^2 \frac{1}{T} \int_1^\infty dt \sin \left[\frac{1}{2}(1+\gamma)xt \right] \cdot (t^{-12} - 2t^{-6}) \quad (46)$$

where $t = r/d_{AB}$ is the dimensionless distance, and the reduced temperature is defined by $T = -1/\beta \epsilon_{AB}$.

In the $k=0$ limit, χ parameter is given by

$$\chi_s = \hat{\chi}(x=0) = \chi_{HT} + \chi_D = \rho C_x [R_{AB}^{-1} \hat{C}_{AA}(0) + R_{AB} \hat{C}_{BB}(0) - 2\hat{C}_{AB}(0)] + 2\beta \rho C_x \hat{V}_{AB}(0, T) \quad (47)$$

As one knows, the second term in the right hand-side of Eq. (47), χ_D , the so-called bare χ parameter is applicable to that of FHLM.

Phase Separation Conditions

The multicomponent polymer blends including block copolymers exhibit a variety of phase separation and transition behaviors.^{11,33} There are unstable macrophases that one can see in the usual binary polymer blends, and metastable or stable microphases by stretch of blocks in block copolymers resulting in the formation of mesophases.

In the light scattering experiments, the intensity, Eq. (48), diverges at each point of the spinodal curve,² and then this leads to a good criterion for phase separations. The inverse scattering intensity can be predicted from the theory as functions of wave-vector and temperature:

$$\hat{I}^{-1}(x, T) \propto \hat{S}_R^{-1}(x, T) = \hat{Q}(x) - 2\hat{\chi}(x, T) \quad (48)$$

In the case of polymer blends with the diblock copolymer, the dominant concentration fluctuation occurs both at $x=0$ and $x=x^*$ of finite characteristic wave-vector. The former gives the spinodal criterion for the macroscopic phase separation between two polymers and the latter gives the criterion for the microphase separation between two blocks of the diblock copolymer.

The spinodal condition for the macrophase separation is then given by

$$\hat{Q}(x=0) - 2\hat{\chi}(x=0, T_s) = 0 \quad (49a)$$

and the spinodal instability for the microphase separation corresponds to

$$\frac{\partial}{\partial x} [\hat{Q}(x) - 2\hat{\chi}(x, T_s) = 0] \Big|_{x=x^*} = 0 \quad (49b)$$

The spinodal conditions for the macro- and microphase separations give χ parameters and temperatures, χ_s and T_s , and χ_s^{macro} and T_s^{micro} , respectively.

The correlation hole effect^{2,12,32} of the scattering function

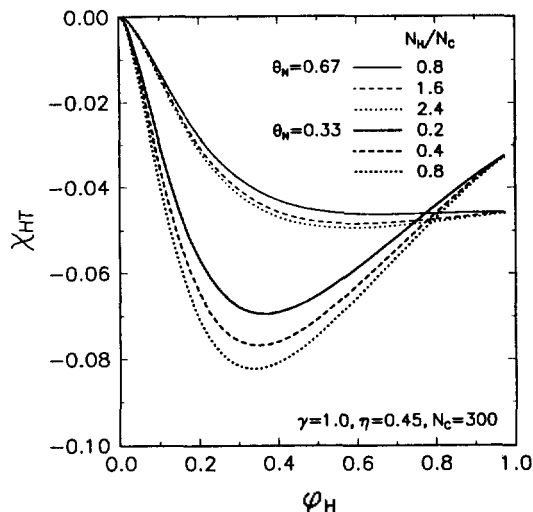


Figure 1. χ parameter at high-temperature limit as a function of ϕ_H in the model A-B/H blends of $\gamma=1.0$, $\eta=0.45$, and $N_C=300$. The composition θ_N of block A in the diblock copolymer A-B is 0.33 (thick lines) and 0.67 (thin lines).

in the polymer blends with block copolymers is caused by the fact that two blocks in the diblock copolymer are strongly stretched at small x because of the connectivity of blocks. This chain stretch results in the conformational entropy loss¹⁷ of blend system in the disordered state and consequently leads to the large free energy as described in Eq. (34). Thus the scattering intensity decreases with decreasing x . In the conventional RPA model, parameter does not show the dependence of wave-vector, and x^* is independent of temperature. However, this work predicts the dependence of x^* on temperature and molecular weight of the diblock copolymer as well.

Results and Discussion

In the FFLM and RPA theory, χ parameter is usually zero or small positive for all athermal mixtures. Figure 1 shows the high-temperature and zero wave vector limits of χ parameter, χ_{HT} in Eq. (37), for the model blends of a diblock copolymer A-B and a homopolymer H (=A). With the exception of nearly zero concentration of the homopolymer, χ_{HT} is negative. In the case of diblock copolymer melt ($\phi_H=0.001$), the calculated χ_{HT} is -0.47×10^{-5} for $\theta_N=0.5$ and $N_H/N_C=1.0$, and 0.38×10^{-4} for $\theta_N=0.33$ and $N_H/N_C=0.2$. χ_{HT} first decreases with ϕ_H and then increases for $\theta_N=0.33$ and levels off for $\theta_N=0.67$ with further increase of ϕ_H . In the fully athermal mixtures, the blend miscibility is strongly enhanced entropically with increasing concentration and chain length ratio for the homopolymer, and also shows the strong dependence of asymmetric structure of the diblock copolymer. At high temperatures the blends may form micelles, such as the uniform solubilization of homopolymer H by block A or block A by homopolymer H. The appearance of minimum point of χ_{HT} in the A-B/H blend system is expected by the formation of structure which is further compatible thermodynamically at the composition of $\theta_N=0.33$. This low χ_{HT} affects 10x parameter at phase separations.

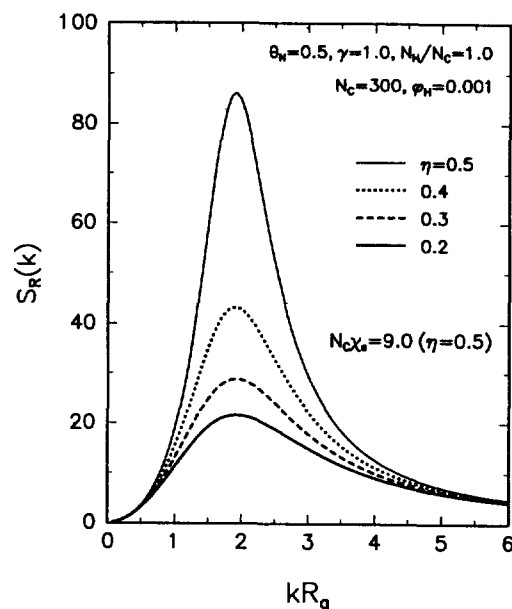


Figure 2. Renormalized RPA-like structure factor $\hat{S}_R(k)$ as a function of kR_g , where the calculations are performed for blends with various packing fractions $\eta=0.2, 0.3, 0.4$, and 0.5 in symmetric blocks of the diblock copolymer, and the same chain length of the homopolymer as that of the diblock copolymer, $N_C=300$, and $\phi_H=0.001$ at $N_C\chi_s=9.0$ for $\eta=0.5$.

Static Scattering Function. To predict the phase separation behaviors in the multicomponent polymer blend systems, the scattering method is a powerful tool. The elastic scattering of light, X-ray, and neutron due to the thermal concentration fluctuations in the disordered states are used to extract χ parameter that provides a gauge of the molecular interaction in the blends. The conventional RPA is one of theories that can be used in relation with the scattering data. But the RPA model has the constraint of incompressibility assumed intrinsically and then χ parameter obtained from the theory has been known not to give the desired molecular interpretation.¹⁷

The renormalized RPA-like structure factor, Eq. (37), obtained from the present theory has the incompressibility condition, Eq. (33b), for the polymers. However, the structure factor in this polymer RISM theory for the A-B/H blend is dependent on the packing fraction since the DCFs as constituent terms of χ parameter are affected by the packing fraction. Even if the packing fraction is taken to be independent of the blend composition, the model blend is compressible.

The renormalized RPA-like structure factor, \hat{S}_R , as a function of kR_g (where R_g is the diblock copolymer radius of gyration) is shown in Figure 2. Where the blends have symmetric blocks of the diblock copolymer of $N_C=300$, and $\phi_H=0.001$. The structure factors are calculated for $\eta=0.2, 0.3, 0.4$, and 0.5 at $N_C\chi_s=9.0$ for $\eta=0.5$. The highly-packed blend shows the strong peak intensity and its height is in the order of increasing η . One can see the similar trend in the compressible RPA work by Tang and Freed.¹⁸

The enhanced miscibility by increasing the concentration of homopolymer leads to lowering of the microphase separa-

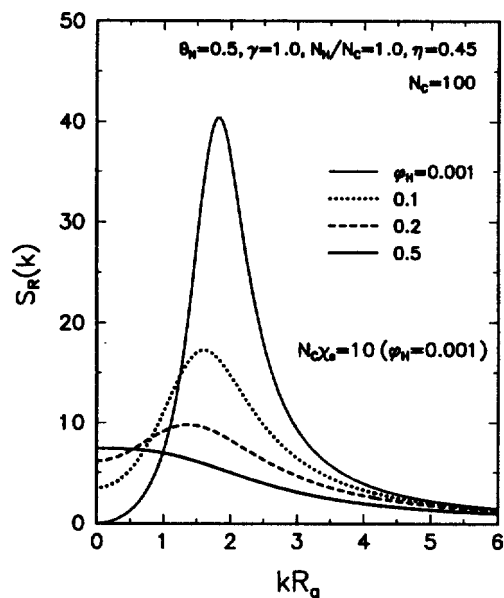


Figure 3. Effect of the added homopolymer on the scattering peak, where the calculation data are for blends containing various volume fractions $\phi_H=0.001, 0.1, 0.2,$ and 0.5 with $N_C=100$ at $N_C\chi_0=10.0$ for $\phi_H=0.001$.

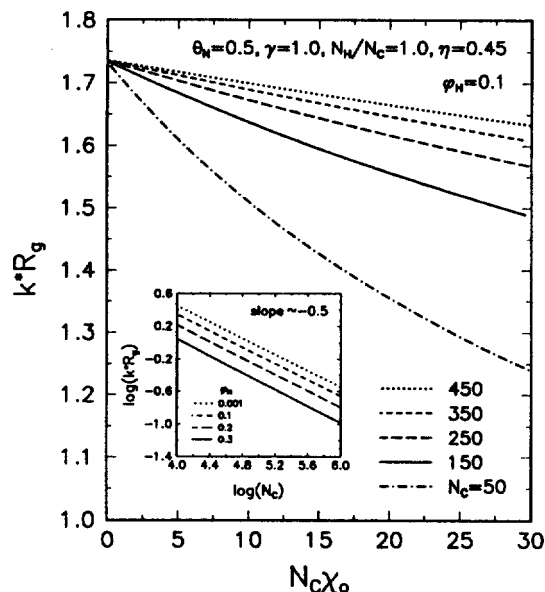


Figure 4. Temperature dependence of the peak wave vector scaled by the radius of gyration R_g in the blend of $\phi_H=0.1$ for $N_C=50, 150, 250, 350,$ and 450 . The inset shows the diblock copolymer N_C -dependence of the scattering peak wave vector for various additions of homopolymer, ϕ_H . The log-log scaled plot for all concentrations of the homopolymer shows the relation of $k^* \propto N_C^{-0.5}$.

tion temperature (MST). The scattering peak wave vector k^* shifts to smaller values and eventually to zero one as the amount of added homopolymer increases. Thus the addition of a sufficient amount of homopolymer causes a phase transition from the microphase separated structure to the macrophase separated one. Such structure factors as a func-

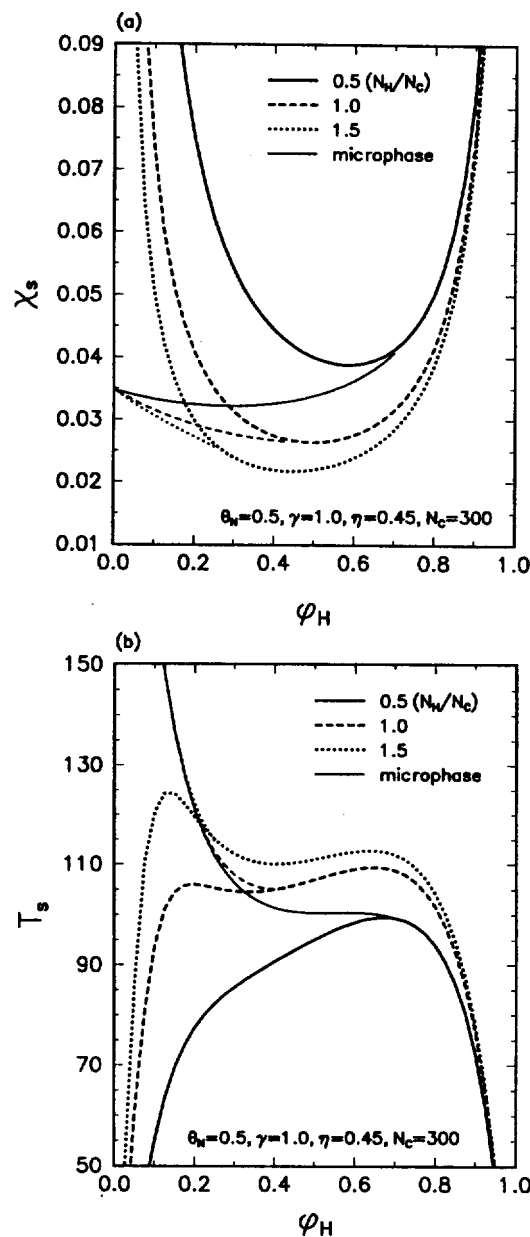


Figure 5. (a) spinodal χ parameter and (b) spinodal temperature T_s as a function of ϕ_H in A-B/H blends with $\theta_H=0.5, \gamma=1.0, \eta=0.45,$ and $N_C=300$ for three ratios of the chain length, $N_H/N_C=0.5, 1.0,$ and 2.0 . The thick and thin lines indicate spinodal curves for the macrophase separation between two polymers and for the microphase separation between two blocks in A-B, respectively.

tion of kR_g are shown in Figure 3. The transition point can be seen for the blend of $\phi_H=0.5$ and $N_C=100$ at the temperature of $N_C\chi_0=10$ for $\phi_H=0.001$.

The temperature dependence of k^* is plotted in Figure 4. The results are similar with the recent data obtained by David and Schweizer³⁷ from the polymer RISM theory with the reference molecular PercusYevik (R-MPY) closure for diblock copolymer melts. Differently with their reference molecular mean-spherical approximation (R-MMA) prediction, here the MSA closure does not predict the minimum

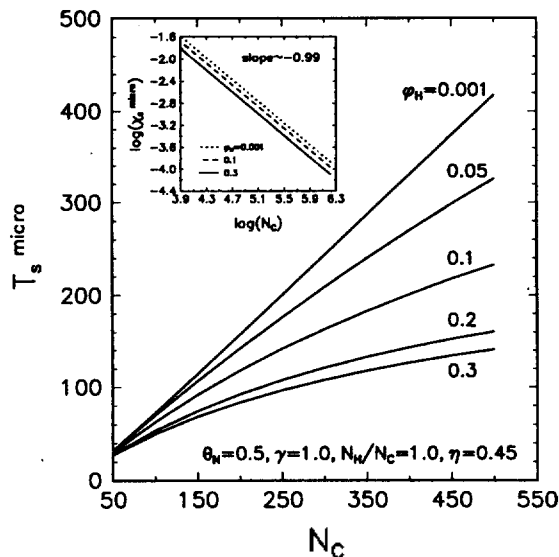


Figure 6. Effect of the added homopolymer on T_s^{micro} as a function of N_C . The inset shows the log-log plot for χ_s^{micro} dependence on N_C at various $\phi_H=0.001, 0.1,$ and 0.3 . The straight lines have the scaling relation of $T_s^{micro} \propto N_C^{1.106}$ at $\phi_H=0.001$ and in the inset $\chi_s^{micro} \propto N_C^{-0.986}$.

for k^* . The calculated k^* decreases steadily with $1/T$. The temperature effect is larger in a smaller N_C .

The inset shows the log-log plot for the scattering peak position on the chain length of the diblock copolymer. For all concentrations of homopolymer, the plot of k^* against N_C reduces to the scaling relation as

$$k^* \propto N_C^{-\delta} \quad \delta \sim 0.5$$

Such a scaling relation is conformable to the result of SANS measurements¹⁵ for the diblock copolymer, poly(ethylene-propylene)-poly(ethylene) (PEP-PEE), by Bates and co-workers.

Spinodal Interaction Parameter χ_s and Temperature T_s . Figures 5(a) and 5(b) show the calculated phase diagrams for χ parameters and reduced temperatures at macro- and microphase separations with increasing of ϕ_H in the blends of the condition of $\gamma=1.0, \eta=0.45,$ and $N_C=300$. Spinodal conditions can be obtained from Eqs. (40a) and (40b) for the macrophase separation [thick curves] and the microphase separation [thin curves], respectively.

In Figure 5(a) the calculated χ_s^{micro} for the model blend system first decreases or increases (even if not shown in here)²⁶ and then increases as the homopolymer is added to the diblock copolymer of $\theta_N=0.5$. This behavior depends on the chain length of the added homopolymer as well as the diblock copolymer composition. In some addition of the homopolymer, the disordered blends transform directly into the instable macrophases without going through the ordered microphases. Such a tendency of the phase separation and transition for χ_s is similar to the result expected by the RPA model.¹¹ The macroscopic spinodal curves in χ_s with ϕ_H are usual phase behaviors such as the binary homopolymer blends.⁴ The spinodal temperatures, however, show different features as shown in Figure 5(b).

According to the RPA, the spinodal temperature plots with

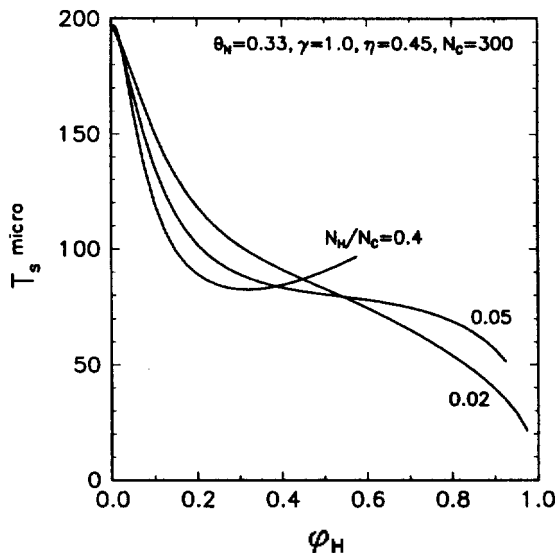


Figure 7. Spinodal temperature T_s^{micro} for the microphase separation as a function of ϕ_H in A-B/H model blends with $\theta_N=0.33, \gamma=1.0, \eta=0.45,$ and $N_C=300$ for three chain length ratios, $N_H/N_C=0.02, 0.05,$ and 0.4 . This figure is compared with the result obtained from SAXS measurements.¹³

ϕ_H have the overturned shapes for the spinodal χ parameters. This appearance may be a result from that the entropy-driven contribution has not been considered effectively with increasing of ϕ_H in total χ parameter, Eq. (13). As shown in Figure 5(b), reduced temperatures T_s^{micro} , which temperature is defined by $T=1/\beta\epsilon_{AB}$, reduce suddenly with addition of a small amount of homopolymer. The feature of minimum points of MST²⁶ at $\phi_H \sim 0.3$ in $\theta_N=0.33$ and the rapid reduction at small ϕ_H correspond to the that of Figure 1.

The MST is usually given by the spinodal temperature as the scattering intensity diverges or by the average interdomain spacing¹³ as decreasing the temperature. For the model blends, $\theta_N=0.5, \gamma=1.0, N_H/N_C=1.0,$ and $\eta=0.45$, the diblock copolymer N_C -dependence, against N_C ranging from 50 to 550, of the MST is plotted in Figure 6. The result is that as increasing N_C, T_s^{micro} increases fair linearly. In the same N_C, T_s^{micro} is lowered by the addition of homopolymer and one can also see the same result in Figure 5(b). In recent calculations performed for the compressible model by the lattice cluster theory (LCT), Dudowicz and Freed¹⁹ predicted the similar N_C -dependence of the order-disorder transition temperature for the diblock copolymer P(S-*b*-MMA) melts. In polymer blends without the homopolymer nearly, the plot of T_s^{micro} with N_C reduces to the scaling relations as

$$T_s^{micro} \propto N_C^{\delta} \begin{cases} \delta=1.106 & \text{in } \phi_H=0.001 \\ \delta=0.0996 & \text{in } \phi_H=0.05 \end{cases}$$

The inset also shows the N_C -dependence of χ_s^{micro} , that is plotted with log-log scale. For all concentrations of homopolymer against N_C ranging from 50 to 500, the relation reduces to the scalingship as

$$\chi_s^{micro} \propto N_C^{-\delta} \quad \delta \sim 0.986$$

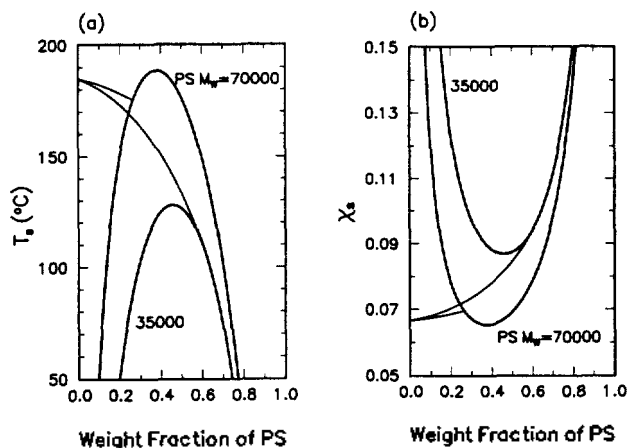


Figure 8. Spinodal temperatures T_s (a) and interaction parameters χ_s (b) for the microphase separation (thin lines) and the macrophase separation (thick lines) as a function of the weight fraction of polystyrene in blends containing the styrene-butadiene copolymer of two block M_w 16850 and 5150, respectively, and polystyrene of two M_w 35000 and 70000. This figure (a) can be found in Roe's systems.¹¹ In terms of our notation, polymer blends have $\theta_N=0.64$, $N_C=300$, and $N_H/N_C=1.32$ and 1.64.

χ_s^{micro} reduces gradually as increasing N_C . This result is also conformable to the result of recent SANS measurements.¹⁶ In spite of high $\phi_H=0.3$, the plot of χ_s^{micro} against N_C in log-log scale gives a straight line, while that of T_s^{micro} against N_C deviates from a straight line.

Comparison of Phase Diagram with Other Results.

Phase behaviors for polymer blends of poly(styrene-*b*-isoprene) block copolymer (SI) and homopolystyrene (HS) are investigated by Hashimoto and co-workers^{12,13} using SAXS measurements. Their T_s^{micro} data as a function of ϕ_H show that the MSTs decrease pronouncedly with increasing amount of the small molecular weight HS. At an increased N_H , the MST decreases with ϕ_H and increases with further addition. The effect of homopolymer on T_s^{micro} as shown in Figure 7 is similar with trends determined by Tanaka and Hashimoto.¹³

Nojima and Roe¹¹ obtained the following results from the extended RPA theory. Figure 8 shows their results for the spinodal temperature (a) and χ parameter (b) as a function of the polystyrene weight fraction. Their model blends contain the polystyrene of molecular weights 70000 and 35000, and the diblock copolymer poly(styrene-*b*-butadiene) of two block weights 16850 and 5150. In the calculations of Figure 8, the interaction energy density Λ is used as

$$\Lambda(\text{cal}/\text{cm}^3) = (0.718 \pm 0.051) - (0.0021 \pm 0.00045)(t - 150 \text{ } ^\circ\text{C})$$

The experimental value for Λ is based on the cloud point curves for the mixtures of polystyrene and polybutadiene or their random copolymer.

Figure 9 shows our results obtained by calculating the extended polymer RISM equations. Any experimental fitting value is not used in this calculations. The polymer blends corresponding to the Roe's systems, in terms of our notation, have a condition of $\theta_N=0.64$, $\gamma=0.86$, $\eta=0.45$, and $N_C=254$. Two chain length ratios are $N_H/N_C=2.65$ and 1.32 for the

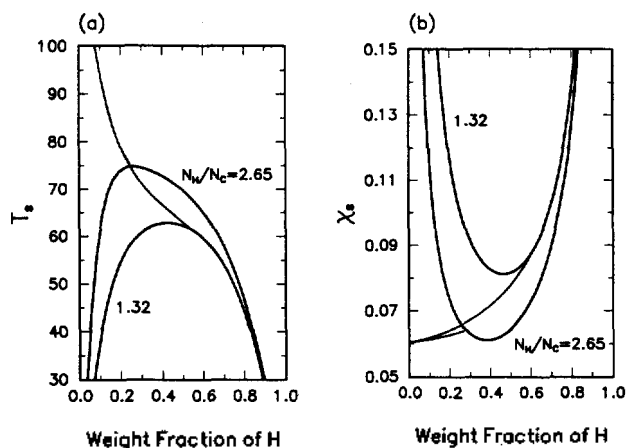


Figure 9. From the polymer RISM theory, calculated spinodal temperatures T_s (a) and interaction parameters χ_s (b) for the microphase separation (thin lines) and the macrophase separation (thick lines) as a function of the weight fraction of polystyrene in blends with $\eta=0.45$ containing the diblock copolymer A-B of $\theta_N=0.64$, $\gamma=0.86$, and $N_C=254$. Two homopolymer chain lengths are $N_H/N_C=1.32$ and 1.64. This figure is compared with Figure 8.

molecular weights 70000 and 35000, respectively. As stressed above, two plots [Figures 7(b) and 8(b)] for χ_s at phase separations with ϕ_H have the same feature each other. This behavior comes from the reason that χ_s is determined by the minimum of $\hat{Q}(k)$ only in Eq. (49). However, two phase diagrams of T_s with ϕ_H [Figures 7(a) and 8(a)] show different behaviors. The MSTs obtained from the polymer RISM reduce more rapidly by small addition of the homopolymer than that obtained from the RPA theory.

In the polymer RISM theory the calculated temperature T_s depends pronouncedly on the choice of intermolecular potential model, Eq. (36). Within the frame of MSA closure, the DCF in the outside of the closest distance of possible approach between segments is given by Eq. (10c). This approximation has been applied fully to the atomic fluids and the small molecular mixtures.^{24,25} But one expects the approximation to be worst at near hard core and also $C_{MM}(r)$ does not in fact approach $-\beta V_{MM}(r)$ asymptotically.²⁵ Moreover, the theory is not exact at low density. Most recently to make up for this problem, Schweizer and co-workers^{37,39,40} presented new closures to the polymer RISM theory, the R-MMSA and R-MPY closures in place of usual MSA and PY closures.

In the polymer RISM theory of A-B/H blend systems, the overestimation may be incorporated to the decreasing tendency of T_s with the addition of homopolymer. In spite of expecting problems, however, the phase diagram obtained from the polymer RISM theory of A-B/H polymer blend with the MSA closure is consistent qualitatively with a recent experimental result for the phase separation spinodal temperatures.

Recently Hellmann and co-workers³³ obtained the phase diagram for T_s with ϕ_H by using transmission electron microscopy (TEM). The polymer blend contains a diblock copolymer P(MMA-*b*-S) of molecular weight 175000 with methyl

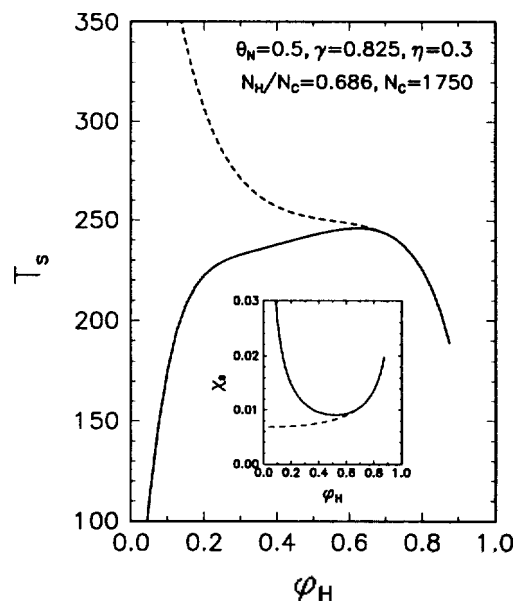


Figure 10. Calculated spinodal temperatures T_s for the microphase separation (dotted line) and the macrophase separation (solid line) as a function of ϕ_H in the blend with $\theta_N=0.5$, $\gamma=0.825$, $\eta=0.3$, $N_H/N_C=0.686$, and $N_C=1750$. The inset shows the spinodal interaction parameters χ_s . This phase diagram is compared with the result by TEM³³ containing a P(MMA-*b*-S) copolymer of M_w 175000 and a PMMA of 161000 (the volume ratio per chain is equal to 0.87).

methacrylate and styrene blocks of equal lengths, and a PMMA homopolymer of molecular weight 161000 ($M_w/M_n=2.0$). The ratio of volume per chain is given by $\lambda (=V_H/V_C)=0.87$. The polymer blend corresponding to the experimental system, in terms of our notation, have a condition of $\theta_N=0.5$, $\gamma=0.825$, $\eta=0.3$, and $N_C=1750$. The chain length ratio is $N_H/N_C=0.686$. The result is shown in Figure 10. This diagram also shows the rapid lowering of MST (the dotted line) with the addition of homopolymer. The temperature and the concentration of homopolymer that the microphase separation does not occur with increasing ϕ_H [critical point] are $T_s^{micro}=100$ °C and $\phi_H=0.7$ in TEM, and $\beta\epsilon_{AB}=-250$ and $\phi_H=0.65$ in our calculation, respectively. One can see that the calculated result are conformable with the experimental one. As above-mentioned, the reduced temperature depends on the choice of the attractive potential model.

Intermolecular Pair Correlation Function. One of the advantages of off-lattice integral equation theories for polymers is that the information about the local structure of the polymer system is available.^{37,39}

The polymer RISM theory provides the local structural informations through the site-site PCFs and the influence of the long wavelength structure for these local properties. Although the phase separated structures do not available from the polymer RISM theory, one can obtain the average pair interactions between any two blend components in the disordered single-phase at a certain distance from the microphase separation point against its athermal reference system. In this section the PCFs are calculated numerically by Eqs. (21) and (28) from the polymer RISM theory with the MSA

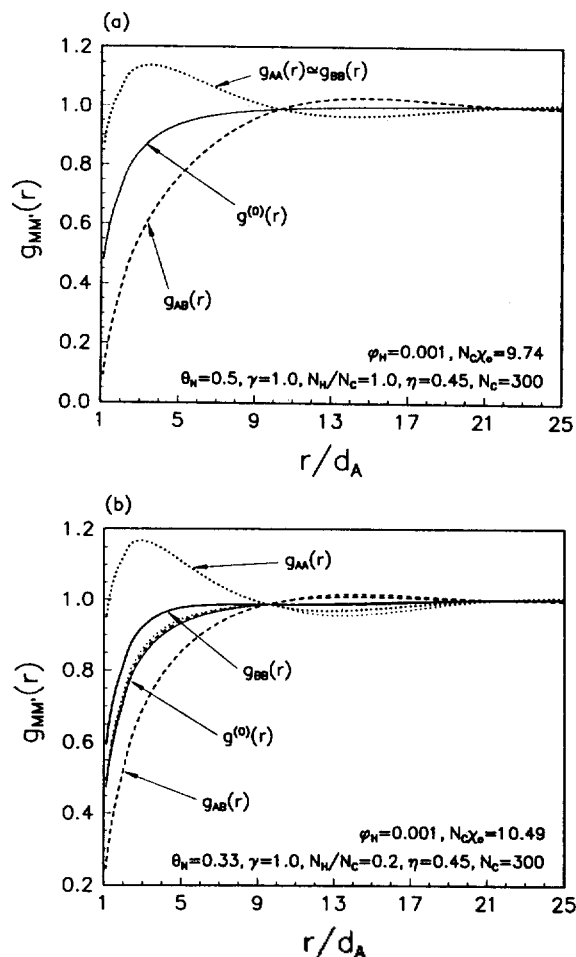


Figure 11. (a) pair correlation functions for the symmetric diblock copolymer with $\phi_H=0.001$ and $N_C=300$ at $N_C\chi_0=9.75$ ($N_C\chi_0^{micro}=10.41$). The folded PCFs are for symmetric blocks of the diblock copolymer as $g_{AA}(r) \cong g_{BB}(r)$ and the solid line indicates the reference blend PCF, $g^{(0)}(r)$, at $T \rightarrow \infty$ limit. (b) Similar to Figure 11(a), but calculated for the asymmetric diblock copolymer, $\theta_N=0.33$, at $N_C\chi_0=10.49$ ($N_C\chi_0^{micro}=12.86$). This figure shows the split PCFs for the reference athermal blend, $g^{(0)}(r)$, and the local structure as $g_{AA}(r) > g_{BB}(r)$.

closure within the frame of Gaussian chain statistics for the model A-B/H blends. We show the calculated results to understand the dependence of PCFs on the block composition of the diblock copolymer and packing fraction related with temperature. These results are not compared with other theories or simulation data, but the PCFs are indebted for facts that the structure factors $\hat{H}_{MM}(k)$ used in calculating the phase separation behaviors and scattering functions are reasonable with experimental results in some measure and previously reported papers.^{11-13,15-19,22,33}

Figure 11(a) shows the PCFs for a nearly symmetric diblock copolymer with $\phi_H=0.001$, and $N_C=300$ at $N_C\chi_0=9.75$ ($N_C\chi_0^{micro}=10.41$). One can see the folded PCFs $g_{AA}(r) \cong g_{BB}(r)$ for symmetric blocks of the diblock copolymer. Here $g^{(0)}(r)$ indicates the site-site PCF in the reference athermal blend (i.e., in high-temperature limit, $T \rightarrow \infty$). At some intermolecular separations the PCFs decrease for A-A and B-B interac-

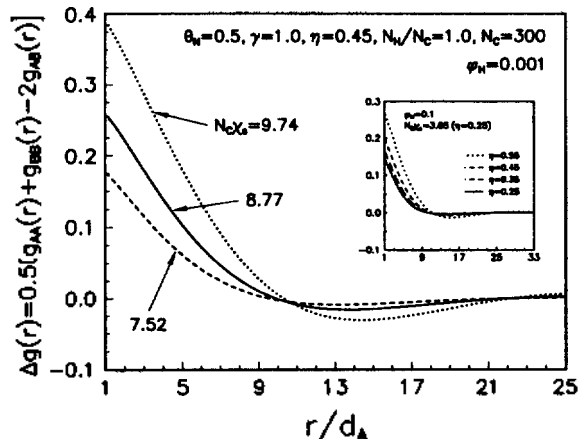


Figure 12. Temperature dependence of the non-randomness $\Delta g(r)$ of intersegment packing for the blend of symmetric diblock copolymer, $N_H/N_C=1.0$, $N_C=300$, and $\phi_H=0.001$. The inset shows the packing fraction dependence of $\Delta g(r)$ for the blend of $\phi_H=0.1$ at $N_C\chi_0=3.65$ for $\eta=0.25$.

tions or increase for the A-B pair interaction, and followed by a slow approach to the uncorrelated value of unity in the range of $r \gg d_A$. However in the $r \leq R_g [= (N_C/6)^{0.5} d_A]$ regime, the local structures show the characteristic features, *i.e.*, the gap between $g_{AA}(r)$ and $g_{AB}(r)$ is very pronounced. The unfavorable contacts between interaction sites of different types cause an increasing in the local packing of like species leading to strong enhanced $g_{AA}(r) > g^{(0)}(r)$ and depleted $g_{AB}(r) < g^{(0)}(r)$.

Figure 11(b) show the PCFs in the asymmetric diblock copolymer of $\theta_N=0.33$, $\phi_H=0.001$, and the length scale of homopolymer $N_H/N_C=0.2$ at $N_C\chi_0=10.49$ ($N_C\chi_0^{micro}=12.86$). The PCFs are also $g_{AA}(r) \neq g_{BB}(r)$ and each PCF in the high-temperature limit reference system does not overlap as like shown in Figure 11(a). In particular one can see the decreasing of favorable contacts between the sites on the long blocks, and then $g_{BB}(r)$ is more depleted and located nearly to $g^{(0)}(r)$ than that of Figure 11(a). These similar features are described recently by David and Schweizer³⁷ by using the R-MPY and R-MMSA closures for block copolymer liquid systems. The asymmetric diblock copolymer system of $\theta_N=0.33$, as shown in Figure 11(b), may form uniform spherical micellar phases in favor of a direction to minimize the number of unfavorable A-B contacts, that is to say, in a way to enhance the local packing of short blocks.

The temperature effect on PCFs as $N_C\chi_0=9.74$, 8.77, and 7.52 is shown in Figure 12 with the same condition as that of Figure 11(a). The favorable local packing of like species is described by the degree of non-randomness $\Delta g(r) \equiv 0.5[g_{AA}(r) + g_{BB}(r) - 2g_{AB}(r)]$ as the qualitative form of the intermolecular PCF. $\Delta g(r)$ approaches to zero at high temperature, however, as lowering temperature $\Delta g(r)$ becomes quite large by the enhancement of local packing correlations between like-pairs inside R_g . In the long distance scales of outside R_g , the polymer blend has the random freely mixing phase as like the athermal reference system. In the same manner, the inset shows the similar results. As increasing the packing fraction, $\Delta g(r)$ also increases in the polymer blend of $\phi_H=0.1$ at $N_C\chi_0=3.65$ for $\eta=0.25$.

The calculated $\Delta g(r)$ for the A-B/H polymer blends from the polymer RISM theory with the MSA closure typically decreases as the separated distance increases. This feature is different from the result of 50/50 isotopic blends with the MSA closure,^{22,41} where plots of $\Delta g(r)$ have maximum points in the medium distance scale, $r \sim R_g/\sqrt{2}$. While on the other, the plot obtained from the same polymer RISM theory with the R-MPY shows the similar our result.

Concluding Remarks

The interaction parameter (function), which is used as a black box in the polymer science, is derived at the molecular level for the polymer blend A-B/H of a diblock copolymer A-B and a homopolymer H by extending the polymer RISM theory with the MSA closure and within the frame of Gaussian statistics. The microscopic χ parameter is obtained as a function that has the dependence of temperature, molecular weight, density, local structure and composition of a diblock copolymer, concentration of a added homopolymer, and even wave vector. The pure entropic part of χ parameter at high temperature limit can be obtained as negative values nearly for all compositions unlike the FHLM that has the zero χ parameter and also the RPA model that needs the experimental data for fitting it.

We calculated χ parameter and the temperature at macro-phase and microphase separations. The obtained phase diagrams are compared with the results obtained from the RPA model¹¹ and TEM experiments.³³ The microphase separation behavior in T_s vs. ϕ_H phase diagram shows the different feature with the RPA, but shows the qualitative consistency with TEM. The MST on the addition of homopolymer shows that it rapidly decreases as increasing the amount of homopolymer and the decreasing effect is large at the short chain of homopolymer. In the case of blend with $\theta_N=0.33$, the MST rapidly decreases at the short chain homopolymer, however, it reduces and then increases at the long chain homopolymer, *i.e.*, the microphase spinodal curve has a minimum point.¹³

The scattering peak position, χ parameter, and temperature at the microphase separation of polymer blends with a symmetric block copolymer have the scaling relationships against a diblock copolymer chain length ranging from 50 to 500, which are given by $k^* \propto N_C^{-0.5}$, $\chi_s^{micro} \propto N_C^{-0.986}$, and $T_s^{micro} \propto N_C$ of $\delta=1.106$ at $\phi_H=0.001$ and $\delta=0.996$ at $\phi_H=0.05$. These scaling relations are conformable to the recent SANS experiments.^{15,16}

We calculated the site-site intermolecular PCFs to investigate the local structure of A-B/H blend. From the PCFs and the non-randomness of blend systems, we expect that the structure is formed to minimize the number of unfavorable A-B contacts, *i.e.*, to enhance the local packing of like-pair of segments such as A-A and B-B. This feature is in line with the results obtained from the MST phase diagrams.

Although the extended polymer RISM theory for A-B/H blend systems has the expecting problems that the polymers follow the Gaussian chain statistics, the MSA closure is used, and the intramolecular and direct intermolecular correlation functions are calculated independently, our calculated results are conformable with the recent experimental data and are more reasonable than that obtained from the conventional FHLM and RPA theory.

Acknowledgment. This study was supported by a grant (95-05-1051) from the SNU-Daewoo Research Fund, 1995.

References

1. Flory, P. J. *Principles of Polymer Chemistry*; Cornell University Press: Ithaca, New York, 1971.
2. de Gennes, P.-G. *Scaling Concepts in Polymer Physics*; Cornell University Press: Ithaca, New York, 1979.
3. (a) Bate, F. S. *Science* **1991**, *251*, 898. (b) Roe, R.-J.; Zin, W.-C. *Macromolecules* **1980**, *13*, 1221.
4. Han, C. D. *Polymer Blends and Composites in Multiphase Systems*; ACS: **1984**, 206.
5. (a) Yoon, K.-S.; Pak, H. *Bull. Korean Chem. Soc.* **1994**, *15*, 45. (b) Yoon, K.-S.; Pak, H.; Lee, J. W.; Chang, T. *ibid.* **1994**, *15*, 214.
6. Miles, I. S.; Rostami, S. *Multicomponent Polymer Systems*; Longman Scientific and Technical 1994.
7. Leibler, L. *Macromolecules* **1980**, *13*, 1602.
8. Fredrickson, G. H.; Helfand, E. *J. Chem. Phys.* **1987**, *87*, 697.
9. Balsara, N. P.; Jonnalagadda, S. V.; Lin, C. C.; Han, C. C.; Krishnamoorti, R. *J. Chem. Phys.* **1993**, *99*, 10011.
10. de la Cruz, M. O.; Sanchez, I. C. *Macromolecules* **1987**, *20*, 440.
11. Nojima, S.; Roe, R.-J. *Macromolecules* **1987**, *20*, 1866.
12. Mori, K.; Tanaka, H.; Hashimoto, T. *Macromolecules* **1987**, *20*, 381.
13. Tanaka, H.; Hashimoto, T. *Macromolecules* **1991**, *24*, 5398.
14. Kim, J. K.; Kimishima, K.; Hashimoto, T. *Macromolecules* **1993**, *26*, 125.
15. Almdal, K.; Rosedale, J. H.; Bates, F. S.; Wignall, G. D.; Fredrickson, G. H. *Phys. Rev. Lett.* **1990**, *65*, 1112.
16. Gehlsen, M. D.; Rosedale, J. H.; Bates, F. S.; Wignall, G. D.; Hansen, L.; Almdal, K. *Phys. Rev. Lett.* **1992**, *68*, 2452.
17. Dudowicz, J.; Freed, K. F. *Macromolecules* **1990**, *23*, 1519.
18. Tang, H.; Freed, K. F. *Macromolecules* **1991**, *24*, 958.
19. Dudowicz, J.; Freed, K. F. *Macromolecules* **1993**, *26*, 213.
20. (a) Binder, K.; Fried, H. *Macromolecules* **1993**, *26*, 6878. (b) Deutsch, H. P.; Binder, K. *ibid.* **1992**, *25*, 6214. (c) Fried, H.; Binder, K. *J. Chem. Phys.* **1991**, *94*, 8349.
21. Huang, T. K.; Balazs, A. C.; Kunz, M. S.; Mayes, A. M.; Russell, T. P. *Macromolecules* **1993**, *26*, 2860.
22. (a) Schweizer, K. S.; Curro, J. G. *J. Chem. Phys.* **1989**, *91*, 5059. (b) Curro, J. G.; Schweizer, K. S. *Macromolecules* **1991**, *24*, 6736; References therein.
23. Lowden, L. J.; Chandler, D. *J. Chem. Phys.* **1973**, *59*, 6587.
24. Hansen, J. P.; McDonald, I. R. *Theory of Simple Liquids*; 2nd ed.; Academic Press: London, 1986.
25. Gray, C. G.; Gubbins, K. E. *Theory of Molecular Fluids*; Clarendon Press: Oxford, 1984; Vol. 1.
26. Lowden, L. J.; Chandler, D. *J. Chem. Phys.* **1974**, *61*, 5228.
27. Chandler, D. *J. Phys., Condens. Matter* **1991**, *3*, F1.
28. Thompson, A. P.; Glandt, E. D. *J. Chem. Phys.* **1993**, *99*, 8325.
29. Curro, J. G.; Schweizer, K. S. *J. Chem. Phys.* **1987**, *87*, 1842.
30. Schweizer, K. S.; Curro, J. G. *Macromolecules* **1988**, *21*, 3070.
31. Schweizer, K. S.; Curro, J. G. *J. Chem. Phys.* **1992**, *96*, 3211; References therein.
32. (a) Leibler, L.; Benoit, H. *Polymer* **1981**, *22*, 195. (b) Benoit, H.; Wu, W.; Benmouna, M.; Mozer, B.; Bauer, B.; Lapp, A. *Macromolecules* **1985**, *18*, 986. (c) Beniot, H.; Benmouna, M.; Wu, W.-L. *ibid.* **1990**, *23*, 1511. (d) Vilgis, T. A.; Benmouna, M.; Benoit, H. *ibid.* **1991**, *24*, 4481.
33. Lowenhaupt, B.; Steurer, A.; Hellmann, G. P.; Gallot, Y. *Macromolecules* **1994**, *27*, 908.
34. (a) Thiele, E. *J. Chem. Phys.* **1963**, *39*, 474. (b) Wertheim, M. S. *Phys. Rev. Lett.* **1963**, *10*, 321.
35. *MinPack-1 Algorithm*; National Technical Information Service U.S. Department of Commerce 1980.
36. (a) Mansfield, M. L. *Macromolecules* **1986**, *19*, 854. (b) Honnel, K. G.; Curro, J. G.; Schweizer, K. S. *ibid.* **1990**, *23*, 3496.
37. David, E. F.; Schweizer, K. S. *J. Chem. Phys.* **1994**, *100*, 7767; **1994**, *100*, 7784.
38. Yoon, K.-S. *Polymer RISM Theory of Diblock Copolymer/Homopolymer Blends, PhD Thesis*; Dept. Chem., SNU, Seoul, 1995.
39. Yethiraj, A.; Schweizer, K. S. *J. Chem. Phys.* **1993**, *98*, 9080.
40. (a) Yethiraj, A.; Schweizer, K. S. *J. Chem. Phys.* **1992**, *97*, 5927. (b) Schweizer, K. S. *Macromolecules* **1993**, *26*, 6033. (c) Schweizer, K. S.; Yethiraj, A. *J. Chem. Phys.* **1993**, *98*, 9053.
41. (a) Schweizer, K. S.; Curro, J. G. *J. Chem. Phys.* **1991**, *94*, 3986. (b) *Chem. Phys.* **1990**, *149*, 105.